ACADEMY OF SCIENCES OF THE USSR
P. N. LEBEDEV PHYSICAL INSTITUTE
Moscow, Leninsky prospect, 53, USSR.

High energy physics
and cosmic rays

Preprint N° 77

O.D.Dalkarov and V.A.Karmanov

# SCATTERING OF LOW ENERGY ANTIPROTONS FROM NUCLEI $^{12}C$ AND $^{16}O$



Moscow 1984

## A b s t r a c t

The differential cross-sections for elastic scattering and cross-sections for exitation of nuclear level by low energy antiprotons from carbon and oxigen nuclei are calculated. Theoretical curves agree with experimental data at 46.8 MeV which have been obtained at LEAR. We predict the differental cross-sections for nuclear level exitation with definite spin projection of exited nucleus. They determine an angular $\gamma$ - quanta distributions in $(\overline{p}, \overline{p}\gamma)$ reactions on nuclei.

In recent experiment which has been fulfiled at LEAR [1] a diffential cross-section of elastic scattering of $\bar{p}$ at 46.8 MeV from nuclei $^{12}C$ and also cross-section for exitation of low lying levels of the residual nucleus were measured. From the experimental data one can conclude that elastic scattering of $\bar{p}$ from nucleus $^{12}C$ at this energy reveals a pronounced diffractive behaviour (in contrast with proton scattering at the same energy). Comparison of the exitation spectra for inelastic scattering of protons and antiprotons shows that the antiproton continuum is substantially smaller than one for $^{12}C(p, p')^{12}C^*$ reaction.

In this paper we show that these data are surprisingly well described by Glauber approximation. This approach as it is known turned out highly successful for description of analogous processes of the scattering of high energy protons and $\pi$ - mesons from nuclei [2]. Antiproton energy in the experiment under investigation is not so high (several tens MeV), therefore it could be expected that at such energies Glauber approximation is not applied. However in this case an amplitude of elementary $\bar{p}p$ scattering (in contrast with pp or $\pi p$ ) has strongly pronounced forward peak, moreover when energy decreases we have a shrinkage of the elastic $\bar{p}p$ forward peak (for comparison the slope of the elastic $\bar{p}p$ forward peak is equal to 35.6 $GeV^{-2}$ at 46.8 MeV [5], at the same time pp elastic cross-section is practically isotropic [6] and slope of pp forward peak at high energy does not exceed the value $\lesssim$ 6 $GeV^{-2}$). An appearance of so narrow forward cone at small energy and its anti-shrinkage behaviour are explained by the fact that at very low

energies several partial waves with nonzero orbital momenta are the ones that contribute. This phenomenon, as it was shown in ref.[3], is not conditioned by the annihilation processes but is determined by the existence of $N\bar{N}$ quasinuclear states with nonzero orbital momenta for relative motion of N and $\bar{N}$ (levels exist practically in all spin-isospin states) [4]. Namely this circumstance leads to substantial enhancement of the partial waves up to $\ell = 3$ in the low energy elastic $\bar{p}p$-scattering. Total number of partial waves (taking into account the different spin-isospin states) is $\gtrsim 20$. The result of a delicate interference between different $\bar{p}p$ partial waves causes the narrow forward cone in $\bar{p}N$ - scattering[3].

The distinctly pronounced forward peak in low energy $\bar{p}N$ - scattering could be a cause that the applicability domain for Glauber approximation is strongly expanded and therefore this approach could be used up to very low energy of incident antiprotons (the latter statement needs, of course, in additional investigation). As for nonadiabatic corrections that a considerable cancellation takes place between nonadiabatic effects and the off-shell effects of the elementary amplitude[7]. Note that the use of Glauber theory for $\bar{p}d$ - scattering at low and medium energy gives rather good results [8].

In Glauber approximation the amplitude of elastic scattering from nucleus A can be represented in the standard form [2]:

$$F_{ii}(q) = ik\int_0^\infty (1 - \exp(i\chi(b)))\, J_0(qb)\, b\, db, \quad (1)$$

where $J_0$ is the Bessel function and

$$\chi(b) = \frac{A}{2\pi k}\int e^{-i\vec{q}\vec{b}} f_N(q)\,\Phi(q)\, d^2q \quad (2)$$

$\phi(q)$ is the elastic nuclear form-factor parametrized (at $4 \leqslant A \leqslant 16$) in the form /9/:

$$\phi(q) = \left(1 - \frac{A-4}{6A} R^2 q^2\right) \exp\left(-\frac{R^2 q^2}{4}\right), \quad (3)$$

$q$ is the momentum transfer, $k$ is the incident hadron momentum. Here $R^2 = 2.50$ fm$^2$ for $^{12}C$ and $R^2 = 2.92$ fm$^2$ for $^{16}O$ /9/. The scattering amplitude on nucleon is of the form

$$f_N(q) = \frac{k\sigma(i+\varepsilon)}{4\pi} e^{-\frac{1}{2}Bq^2} \quad (4)$$

At the energy $E_{\bar{p}} = 46.8$ MeV we use the following parameters for $\bar{p}N$ - amplitude /5,10/: $\sigma_{\bar{p}p} = 240$ mb, $\sigma_{\bar{p}n} = 200$ mb, $\varepsilon_{\bar{p}p} = \varepsilon_{\bar{p}n} = -0.25$, $B_{\bar{p}p} = B_{\bar{p}n} = 35.6$ (GeV/c)$^{-2}$ $= 1.4$ fm$^2$. The value of $\sigma_{\bar{p}n}$ was found from the cross-section $\sigma_{\bar{p}d} = 380$ mb /11/ taking into account the Glauber correction for screening /2/.

The amplitude of inelastic scattering with exitation of nuclear level of natural parity with spin $J$ and its projection M on the direction of incident beam is expressed in the one-step inelastic collision approximation in terms of electromagnetic transition form-factor and elastic scattering amplitude /12/. It is conveniently to transform the expression for amplitude obtained in ref./12/ to the following form

$$F_{fi}^{M}(q) = \frac{2\sqrt{\pi}}{\sqrt{2J+1}} A f_N(0)(-1)^M Y_{JM}^*\left(\frac{\pi}{2}, 0\right) \int_0^\infty \tilde{S}_{JM}(b) e^{i\chi(b)} J_M(qb) b\,db \quad (5)$$

where

$$\tilde{S}_{JM}(b) = \int_0^\infty S_J(q) e^{-\frac{1}{2}Bq^2} J_M(qb)\, q\, dq \quad (6)$$

$S_J(q)$ determines an inelastic transition form-factor and is parametrized in the form

$$S_J(q) = q^J(a_1 + b_1 q^2 + c_1 q^4)e^{-\alpha q^2}, \qquad (7)$$

that allows to calculate the integral (6) analytically (see Appendix I). The parameters in (7) are known from inelastic scattering electron data. We used the following their values. For exitation of $2^+$(4.44 MeV) level for nucleus $^{12}C$ (see ref./13/): $a_1 = 0.25$, $b_1 = -0.021$, $c_1 = 0.0004$, $\alpha = 0.54$ (in formula (7) $q$ is in $fm^{-1}$). For exitation of $3^-$(6.13 MeV) level for nucleus $^{16}O$ (see ref. /14/): $a_1 = 0.195$, $b_1 = -0.008$, $c_1 = 0$, $\alpha = 0.8125$. In formulae (2) and (5) the difference of scattering amplitude on proton and neutron was taken into account, i.e. the phase $\chi(b)$ was defined as half sum of expressions (2) with $\bar{p}p$ and $\bar{p}n$ amplitudes and the amplitude $F^M_{fi}(q)$ was the corresponding half sum of expressions (5). The amplitudes (1) and (5) were multiplied by the factor $exp(q^2R^2/4A)$ taking into account the recoil of nucleus. For comparison the calculations of the proton scattering at the same energy from $^{12}C$ were made with the following parameters of $\bar{p}N$ amplitudes /6/: $\sigma_{pp} = 44$ mb, $\sigma_{pn} = 204$ mb, $\varepsilon_{pp} = 1.85$, $\varepsilon_{pn} = 0.25$, $B_{pp} = B_{pn} = 0$.

In fig.1 the elastic $\bar{p}^{12}C$ and $p^{12}C$ cross sections are shown. It is seen that our calculation of $\bar{p}^{12}C$ cross section (solid curve) agrees fairly well with antiproton data. On the other hand, the calculated proton cross section (dashed curve) strongly differs from the experimental data /1/. In our opinion, this fact confirms that good description of the antiproton data by Glauber theory is

no more chance, but natural consequence of unusually narrow forward cone in $\bar{p}N$ - scattering. In fig.1 we show also a prediction for elastic antiproton scattering from $^{16}O$ (dash-dotted curve).

In fig.2 by the solid curves the function $\Gamma(b) = 1 - \exp(i\chi(b))$, which determines by eq.(1) the elastic $\bar{p}^{12}C$ scattering amplitude is shown. The dashed curves in fig.2 correspond to $\Gamma(b)$ for $p^{12}C$ scattering. The value $\Gamma(b) = 1$ corresponds to absolutely black nucleus. It is seen that both for the incident antinucleon and for nucleon the nucleus is a black (in the central region) sphere with the diffuse surface. Due to this reason the $\bar{p}N$ amplitude spin structure appeares to be not important for our calculations of antiproton-nucleus cross sections. Note that this spin structure is rather essential in the case of $\bar{p}N$ scattering.

Let us find the effective radius $R_{eff}$ of the black nucleus. The cross section of scattering from black sphere of radius $R_{eff}$ has the form

$$\frac{d\sigma}{d\Omega} = \frac{k^2 R_{eff}^2}{q^2} J_1^2(q R_{eff}) . \qquad (8)$$

We define the radius $R_{eff}$ by the requirement of equality of the cross section (8) at $\theta = 0^\circ$ and the amplitude (1) modulus squared. Note that the formula (8), as well as Glauber formula (1), are valid provided $kR_{eff} \gg 1$. From eqs.(1) and (8) we find

$$R_{eff}^2 = 2\left| \int_0^\infty \Gamma(b)\, b\, db \right| \qquad (9)$$

For $\bar{p}^{12}C$ scattering we obtain $R_{eff} = 3.96$ fm, that corresponds to the parameter $r_0$ in the formula $R = r_0 A^{1/3}$ equaled

to 1.73 fm in comparison with usually accepted value $r_0$ = 1.15 fm and R = $1.15 \cdot 12^{1/3}$ = 2.63 fm. For $p^{12}C$ scattering we obtain $R_{eff}$ = = 3.06 fm. Appreciably greater effective radius for $\bar{p}^{12}C$ scattering is connected with large value of the parameter $B_{\bar{p}N}$ in the amplitude (4), i.e. with strong domination of the forward $\bar{p}N$ scattering.

The elastic $\bar{p}^{12}C$ cross section calculated in the framework of the black nucleus model with sharp surface (eq.(8)) at $R_{eff}$ = 3.96 fm is shown in fig.1 (dotted curve). This model exactly reproduces the $\bar{p}^{12}C$ cross section up to the first minimum ( $q \lesssim 1$ fm$^{-1}$) inspite of the fact that the parameter $kR_{eff}$ = 5.5 is not asymptotically large in the case of $\bar{p}^{12}C$ scattering (but greater than the value $kR_{eff} \approx 4$ for $p^{12}C$ scattering). This calculation overestimates the experimental data at $q >$ 1 fm$^{-1}$ due to strong diffraction from sharp surface.

Total cross-section for $\bar{p}^{12}C$ interaction could be expressed using the function $\Gamma(b)$ by the following formula

$$\sigma_{tot} = \frac{4\pi}{k} Im F_{el}(0) = 4\pi \int_0^\infty Re\,\Gamma(b)\, b\, db$$

As it is seen from Fig.2, $Re\,\Gamma(b) \gg Im\,\Gamma(b)$, therefore $\sigma_{tot} = 2\pi R_{eff}^2$, where $R_{eff}$ is determined by Eq.(9). For the value $R_{eff}$, calculated above, we obtain: $\sigma_{tot}$ = 984 mb. The integrated elastic cross-section beyond 5° (by Eq.(8) ) is found to be $\sigma_{el}$ = 464 mb in agreement with the experimental value $\sigma_{el}^{exp}$ = 450 ± 55 mb (see ref. /1/). Note that in our calculations the reaction cross-section $\sigma_r = \sigma_{tot} - \sigma_{el}$ should be equal to $\sigma_r = \pi R_{eff}^2$ = 492 mb in distinct disagreement with the predictions of optical potentials (in accordance to which $\sigma_r$ = = 620 ± 10 mb /1/ ).

In fig.3 the inelastic (with exitation of $2^+$(4.44 MeV)-level) $\bar{p}^{12}C$ and $p^{12}C$ cross sections are shown. The theory (solid curve) describes rather well the antiproton data. In the case of the proton data the calculation (dashed curve) does not agree with experiment /1/, as well as for the elastic $p^{12}C$ scattering.

A certain excess in fig.3 of the antiproton data over the theory at $\theta > 35°$ ( $q > 0.8$ fm$^{-1}$) can be connected in particular, with the following reasons: (a) with uncertainties in the transition form-factor (7); (b) with inaccuracy of Glauber approximation for large angle scattering; (c) with the collective nature of the exited $2^+$ level and with inapplicability in this case of the one-step inelastic collision approximation. In connection with the possibility (c) we note that the model considering the $2^+$(4.44 MeV) level as collective (rotational) one increases the calculated $p^{12}C$ inelastic cross section at energy 1 GeV (see /15/ ) in comparison with the shell model calculation /9/ and leads to better agreement with experiment. Analogous excess the experimental data /16/ over the calculation /17/ (in the framework of the one-step inelastic collision approximation) at angles beyond the cross section maximum was found also in the cross section of exitation of $3^-$(6.13 MeV) - level in $^{16}O$ by the high energy $\pi^+$ mesons. This discrepancy was eliminated by the model, in which the $3^-$(6.13 MeV) level has the rotational nature. The calculation /17/ was carried out in the framework of the complete Glauber theory, without the one-step inelastic collision approximation. In this connection the analogous study of the influence of the nuclear structure on the antiproton-nuclei interactions would be of considerable interest.

It should be mention that the inelastic scattering amplitude (5) is rather sensitive to the nuclear surface /12/. Indeed, the factor $exp(i\chi(b)) = 1 - \Gamma(b)$ in the amplitude (5) equals to zero inside a nucleus and to 1 outside it. On the contrary, the function $\tilde{S}_{JM}(b)$ decreases rapidly outside a nucleus. Consequently the integral (5) is determined by the overlaping region near the nuclear surface. Therefore the black sphere model with sharp surface gives rather rough description of the inelastic cross section and underestimates the result by 2-3 times.

In fig.3 we show also the predictions for antiproton inelastic cross sections with definite spin projection M of exited nucleus on the beam direction (M equals to 0 and 2, $\frac{d\sigma}{d\Omega} = \frac{d\sigma_0}{d\Omega} + 2\frac{d\sigma_2}{d\Omega}$, according to eq.(5) $\frac{d\sigma_1}{d\Omega} = 0$ at $J = 2$). It is seen, that these cross sections have a peculiar angular dependence. Their measurement would be a more detailed test of the theory.

The cross section $d\sigma_M/d\Omega$ can be easy obtained from angular distributions of $\gamma$ - quanta emitted in transition of excited nucleus to the ground state. For high energy $\pi^+$ - mesons and protons interacting with $^{16}O$ nucleus such experiments have been carried out (see refs./16/), the data /16/ were partially cited in ref./17/). The angular distribution of $\gamma$ - quanta is determined by the polarization density matrix of excited nucleus:

$$\rho_{MM'}(\vec{q}) = \frac{F_{fi}^{M}(\vec{q})\, F_{fi}^{*M'}(\vec{q})}{\sum_{M} \left| F_{fi}^{M}(\vec{q}) \right|^2} \qquad (10)$$

From eqs.(5) and (6) it follows:

$$\rho_{MM'} = \rho_{-M,-M'}\,, \quad \rho_{M,-M'} = (-1)^{M'}\rho_{MM'}\,, \quad \rho_{-M,M'} = (-1)^{M}\rho_{MM'}$$

Therefore for the levels with $J = 2$ and $J = 3$ the density matrix is determined by three independent elements only: $\rho_{00}, \rho_{22}, \rho_{20}$ for $J = 2$ and $\rho_{11}, \rho_{33}, \rho_{31}$ for $J = 3$ (according to eq.(5) the amplitude $F_{fi}^{M}(q)$ differs from zero only for projections M having the same parity as spin $J$ ). The angular distribution of $\gamma$ - quanta emitted in the transition $J \to 0$ can be obtained from the formula:

$$W(\theta_\gamma, \varphi_\gamma, \vec{q}) = \sum_{MM'} \rho_{MM'}(\vec{q}) \vec{Y}_{JM}^{(\lambda)}(\theta_\gamma, \varphi_\gamma) \vec{Y}_{JM'}^{*(\lambda)}(\theta_\gamma, \varphi_\gamma) , \qquad (11)$$

where $\vec{Y}_{JM}^{(\lambda)}(\theta_\gamma, \varphi_\gamma)$ is well known photon spherical vector, $\theta_\gamma$ is the angle between the beam and $\gamma$ - quantum momenta, $\varphi_\gamma$ is the angle between the plane formed by these two momenta and the scattering plane $(\bar{p}, \bar{p}')$. Explicit expressions for the angular distributions of $\gamma$ - quanta emitted in the deexcitation process of nuclei with $J = 2$ and $J = 3$ are given in Appendix II.

The results of analogous computations of $\bar{p}^{12}C$ cross sections for different energies of incident antiprotons are presented in the Table (the choice of energy was determined by availability of the required exprerimental data on $\bar{p}N$ amplitudes).

In fig.4 the predictions for the reaction $\bar{p}^{16}O \to \bar{p}^{16}O^*$ ($3^-$, 6.13 MeV) cross section are shown. Note that the magnitude of the cross section $d\sigma_1/d\Omega$ in the first maximum three times exceeds the cross section in the second maximum, whereas in the case of the high energy hadron scattering the first maximum is practically unobserved (it is by 10-30 times smaller than the second maximum, see figs. 6-9 in ref.[17]).

By this way, as it follows from the figures, the theoretical curves well agree with the antiproton data available. The antipro-

ton-nucleon amplitude parameters will be measured in the near future with good accuracy at LEAR. In its turn this will allow to calculate more precisely the antiproton-nucleus cross sections.

The authors are sincerely grateful to Prof.I.S.Shapiro for his encouragement continuing interest and stimulating discussions.

## APPENDIX I

The expressions for function $\tilde{S}_{JM}(\delta)$ defined by the formula (6) are given below. We introduce the following notations: $\gamma = \alpha + \frac{\beta}{2}$, $z = \frac{\delta^2}{4\gamma}$ (the definitions of $\beta$ and $\alpha$ are contained in Eqs.(4) and (7) ).

(a) Spin of nucleus $J = 2$, projections $M = 0$ and $M = 2$:

$$\tilde{S}_{20}(\delta) = \frac{e^{-z}}{2\gamma^2}\left[a_1(1-z) + \frac{2b_1}{\gamma}\left(1-2z+\frac{1}{2}z^2\right) + \right.$$
$$\left. + \frac{6c_1}{\gamma^2}\left(1-3z+\frac{3}{2}z^2-\frac{1}{6}z^3\right)\right] \qquad (12)$$

$$\tilde{S}_{22}(\delta) = \frac{z\,e^{-z}}{2\gamma^2}\left[a_1 + \frac{3b_1}{\gamma}\left(1-\frac{1}{3}z\right) + \right.$$
$$\left. + \frac{12c_1}{\gamma^2}\left(1-\frac{2}{3}z+\frac{1}{12}z^2\right)\right] \qquad (13)$$

(b) Spin of nucleus $J = 3$, projections $M = 1$ and $M = 3$:

$$\tilde{S}_{31}(\delta) = \gamma^{-\frac{5}{2}} z^{\frac{1}{2}} e^{-z}\left[\left(1-\frac{1}{2}z\right)a_1 + \frac{3b_1}{\gamma}\left(1-z+\frac{1}{6}z^2\right) + \right.$$
$$\left. + \frac{12c_1}{\gamma^2}\left(1-\frac{3}{2}z+\frac{1}{2}z^2-\frac{1}{24}z^3\right)\right] \qquad (14)$$

$$\tilde{S}_{33}(\delta) = \frac{1}{2}\gamma^{-\frac{5}{2}} z^{\frac{3}{2}} e^{-z}\left[a_1 + \frac{4b_1}{\gamma}\left(1-\frac{1}{4}z\right) + \right.$$
$$\left. + \frac{20c_1}{\gamma^2}\left(1-\frac{1}{2}z+\frac{1}{20}z^2\right)\right] \qquad (15)$$

Let's remind that in accordance with /14/ the coefficient $C_1$ in formulae (14) and (15) can be put to zero.

## APPENDIX II

The angular distribution normalized to unity for $\gamma$ - quanta emitted from nucleus with $J = 2$, in transition to the state with $J = 0$ has the form

$$W(\theta_\gamma, \varphi_\gamma, \vec{q}) = \frac{5}{8\pi}\Big[\rho_{00}(q)\,3\sin^2\theta_\gamma\cos^2\theta_\gamma + \\ + \rho_{22}(q)(1-\cos^4\theta_\gamma - \sin^4\theta_\gamma\cos 4\varphi_\gamma) - \\ - Re\,\rho_{20}(q)\,2\sqrt{6}\sin^2\theta_\gamma\cos^2\theta_\gamma\cos 2\varphi_\gamma\Big] \qquad (16)$$

We have made use of the relation $\rho_{2,-2} = \rho_{22}$.

For $3 \longrightarrow 0$ transition we find

$$W(\theta_\gamma, \varphi_\gamma, \vec{q}) = \frac{7}{2^7\pi}\Big\{15\rho_{33}(q)\Big[1-\cos^2\theta_\gamma - \\ - \cos^4\theta_\gamma + \cos^6\theta_\gamma - \sin^6\theta_\gamma\cos 6\varphi_\gamma\Big] + \\ + \rho_{11}(q)\Big[(1+111\cos^2\theta_\gamma - 305\cos^4\theta_\gamma + 225\cos^6\theta_\gamma) - \\ -(1-130\cos^2\theta_\gamma + 225\cos^4\theta_\gamma)\sin^2\theta_\gamma\cos 2\varphi_\gamma\Big] + \\ + 2\sqrt{15}\,Re\,\rho_{31}(q)\sin^2\theta_\gamma\Big[(15\cos^4\theta_\gamma - 6\cos^2\theta_\gamma - 1)\cos 2\varphi_\gamma + \\ + (1-15\cos^2\theta_\gamma)\sin^2\theta_\gamma\cos 4\varphi_\gamma\Big]\Big\} \qquad (17)$$

Here we have made use of the relations

$$\rho_{1,-1} = -\rho_{11}, \quad \rho_{3,-3} = -\rho_{33}, \quad \rho_{3,-1} = -\rho_{31}.$$

The distributions (16) and (17) integrated over azimuthal angle $\varphi_\gamma$ are determined only by the cross sections $d\sigma_M/d\Omega$ shown in Figs. 3 and 4 and listed in Table and are coincided with the expressions obtained in ref./18/.

## REFERENCES


1. D.Garreta, P.Birion, G.Bruge et al. Phys. Lett. 135B (1984) 266; CERN Courier, 23 (1983) 416.
2. R.Glauber. Uspekhi Fiz. Nauk 103 (1971) 641; V.M.Kolybasov, M.S.Marinov. Uspekhi Fiz. Nauk 109 (1973) 137.
3. O.D.Dalkarov, F.Myhrer. Nuovó Cimento 40A (1977) 152.
4. I.S.Shapiro. Phys. Rep. 35C (1978) 129.
5. $\bar{N}N$ and $\bar{N}D$ Interactions - A Compilation, LBL-58, 1972.
6. A.K.Kerman, M.Mc.Manus and R.M.Thaler. Ann. Phys. 8 (1959) 551.
7. O.D.Dalkarov, V.M.Kolybasov and V.G.Ksenzov. Nucl. Phys. A397 (1983) 498.
8. L.A.Kondratyuk, M.Zh.Shmatikov, R.Bidzarri. Yad. Fiz. (Sov. Jorn. Nucl. Phys.) 33 (1981) 795.
9. R.H.Bassel, C.Wilkin. Phys. Rev. 174 (1968) 1179.
10. M.Cresti, L.Peruzzo, G.Sartori. Phys. Lett 132B (1983) 209.
11. R.D.Tripp, in Proceedings of the $5^{th}$ European Symposium on Nucleon-Antinucleon Interactions, Bressanone (Italy), 23-28 Jine 1980, p.519.
12. V.V.Balashov. Proc. of $8^{th}$ Winter School LINP, part II, p.255, Leningrad, 1973; V.N.Mileev, T.V.Mishchenko. Phys. Lett. 47B (1973) 197; L.A.Kondratyuk, Yu.A.Simonov. Pisma ZhETF (JETP Lett.) 17 (1973) 619.
13. M.Bouten, P.van Leuven. Ann. Phys. 43 (1967) 421.
14. S.I.Manaenkov. Pisma ZhETF (JETP Lett.) 19 (1974) 593.
15. A.N.Antonov, E.V.Inopin. Yad. Fiz. (Sov. Journ. Nucl. Phys.) 16 (1972) 74.

16. I.V.Kirpichnikov, V.A.Kuznetsov, I.I.Levintov, A.S.Starostin. Preprint ITEP-96, Moscow 1979 (in Russian);
I.V. Kirpichnikov, V.A.Kuznetsov, A.S.Starostin. Preprint ITEP-119, Moscow 1981 (in Russian).

17. V.A.Karmanov. Yad. Fiz. (Sov. Journ. Nucl. Phys.) 35 (1982) 948.

18. S.I.Manaenkov. Yad. Fiz. (Sov. Journ. Nucl. Phys.) 20 (1974) 677.

## FIGURE CAPTIONS

Fig. 1 Differential elastic cross sections for $\bar{p}^{12}C$, $p^{12}C$ and $\bar{p}^{16}O$ - scattering at E = 46.8 MeV. Dotted curve was calculated in the framework of black nucleus model with sharp surface (eq.(8) at $R_{eff}$ = 3.96 fm). The experimental data are taken from ref. /1/.

Fig. 2 The function $\Gamma(b) = 1 - exp(i\chi(b))$. Solid curves 1 and 2 are $Re\,\Gamma(b)$ and $Im\,\Gamma(b)$ correspondingly for $\bar{p}^{12}C$ - scattering. Dashed curves 1 and 2 are the same for $p^{12}C$ scattering.

Fig. 3 Inelastic (with exitation of $2^+$(4.44 MeV) - level) differential cross sections for $\bar{p}^{12}C$ and $p^{12}C$ scattering at E = 46.8 MeV. Dotted curves are the cross sections $d\sigma_0/d\Omega$ and $d\sigma_2/d\Omega$ with definite spin projections M (M = 0 and 2) of $^{12}C^*(2^+)$ - nucleus on beam direction ($d\sigma/d\Omega = d\sigma_0/d\Omega + 2\,d\sigma_2/d\Omega$). The experimental data are from ref. /1/.

Fig. 4 Inelastic (with exitation of $3^-$(6.13 MeV) - level) differential cross section for $\bar{p}^{16}O$ - scattering at E = 46.8 MeV. Dotted curves are the cross sections $d\sigma_1/d\Omega$ and $d\sigma_3/d\Omega$ with definite spin projections M (M = 1 and 3) of $^{16}O^*(3^-)$ - nucleus on beam direction ($d\sigma/d\Omega = 2\,d\sigma_1/d\Omega + 2\,d\sigma_3/d\Omega$).

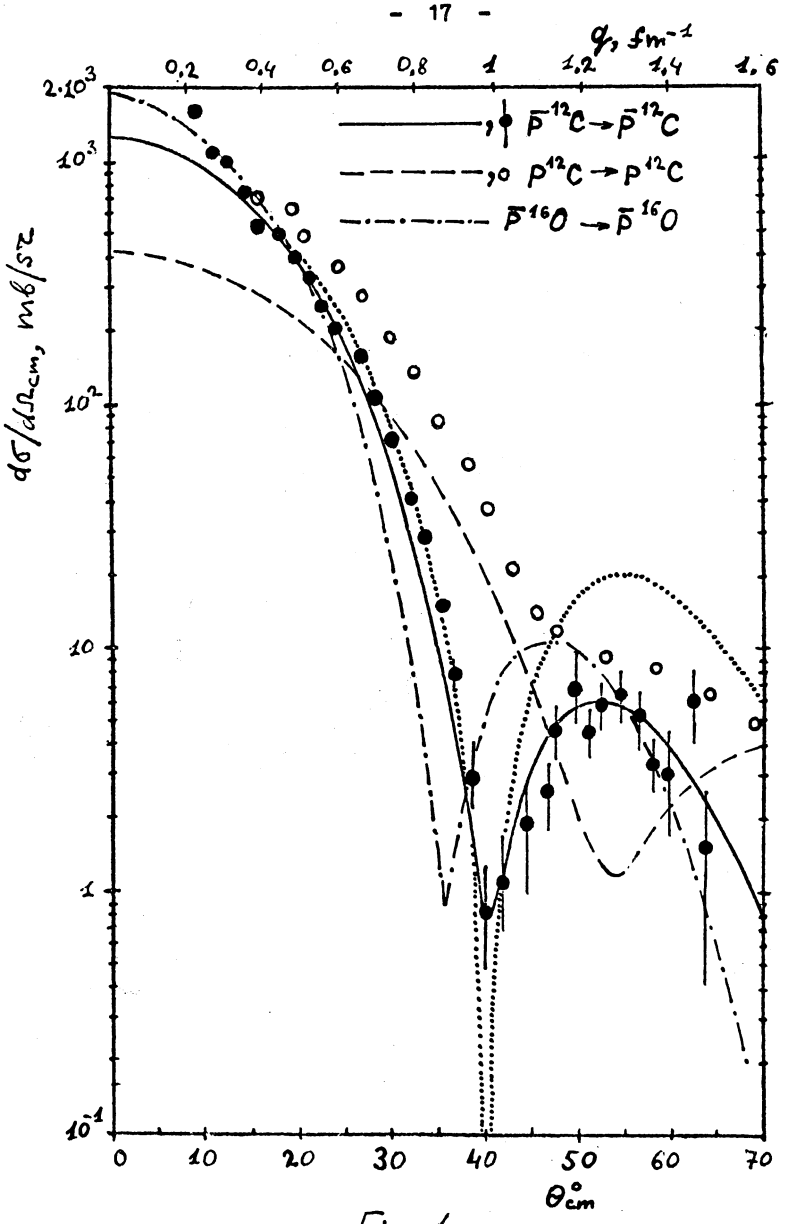
q, fm⁻¹
0,2
0,4
0,6
0,8
1
1,2
1,4
1,6
2·10³
10³
10²
10
1
10⁻¹
dσ/dΩcm, mb/sr
p̄ ¹²C → p̄ ¹²C
p ¹²C → p ¹²C
p̄ ¹⁶O → p̄ ¹⁶O
0
10
20
30
40
50
60
70
θ°cm

Fig. 1

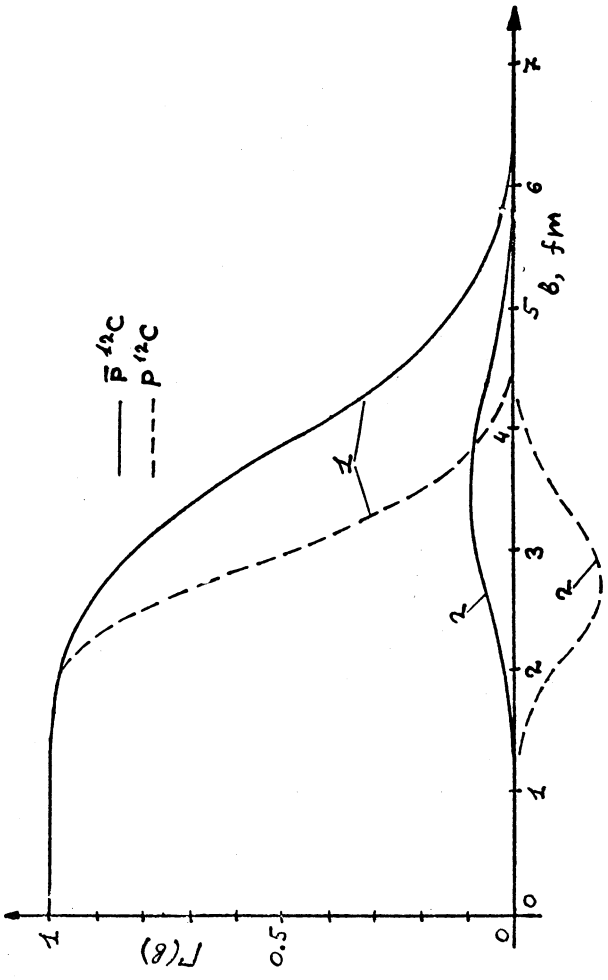


Fig. 2

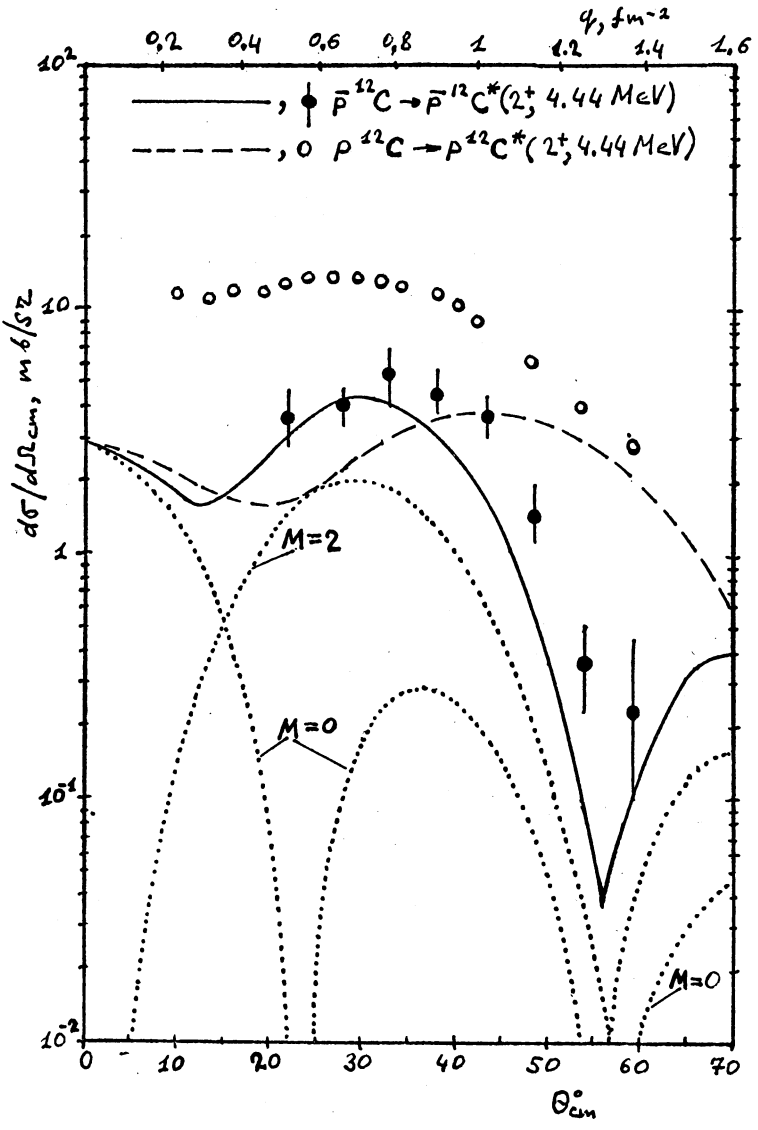
q, fm⁻²
0,2
0,4
0,6
0,8
1
1,2
1,4
1,6
10²
10
1
10⁻¹
10⁻²
dσ/dΩcm, mb/sr
p̄ ¹²C → p̄ ¹²C*(2⁺; 4.44 MeV)
p ¹²C → p ¹²C*(2⁺; 4.44 MeV)
M=2
M=0
M=0
0
10
20
30
40
50
60
70
θ°cm

Fig. 3

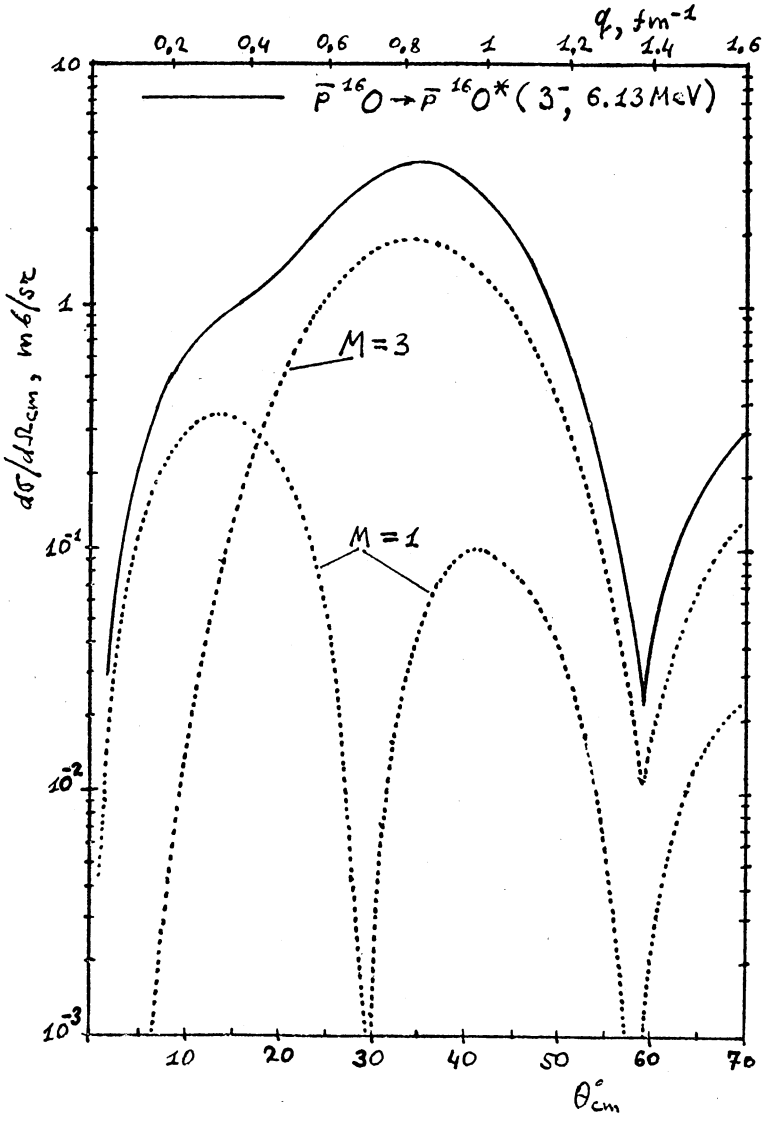
q, fm⁻¹
0,2
0,4
0,6
0,8
1
1,2
1,4
1,6
$\bar{p}\,^{16}O \to \bar{p}\,^{16}O^*(3^-, 6.13\,MeV)$
M=3
M=1
dσ/dΩcm, mb/sr
10
1
10⁻¹
10⁻²
10⁻³
10
20
30
40
50
60
70
θ°cm

Fig. 4

Table

The cross sections of elastic and inelastic antiproton scattering from $^{12}C$

| Energy | Parameters for $\bar{p}N$-amplitudes | Angle | Elastic scattering | Inelastic scattering (with exitation of $2^+$(4.44 MeV)-level | | |
|---|---|---|---|---|---|---|
| | | $\theta^\circ_{cm}$ | $\frac{d\sigma^{el}}{d\Omega_{cm}}, \frac{mb}{sr}$ | $\frac{d\sigma}{d\Omega_{cm}}, \frac{mb}{sr}$ | $\frac{d\sigma_0}{d\Omega_{cm}}, \frac{mb}{sr}$ | $\frac{d\sigma_2}{d\Omega_{cm}}, \frac{mb}{sr}$ |
| E = 64.1 MeV | $\sigma_{\bar{p}p}$ = 221 mb, $\sigma_{\bar{p}n}$ = 181 mb<br>$B_{\bar{p}p} = B_{\bar{p}n}$ = 33.5 (GeV/c)$^{-2}$<br>$\varepsilon_{\bar{p}p} = \varepsilon_{\bar{p}n}$ = -0.22 | 5 | I.40E+3 | 2.87E+0 | 2.82E+0 | 2.36E-2 |
| | | I0 | I.05E+3 | 2.08E+0 | I.47E+0 | 3.06E-I |
| | | I5 | 6.3IE+2 | 2.54E+0 | 3.56E-I | I.09E+0 |
| | | 20 | 2.96E+2 | 4.I6E+0 | 4.I8E-4 | 2.08E+0 |
| | | 25 | 9.76E+I | 5.38E+0 | I.69E-I | 2.60E+0 |
| | | 30 | I.7IE+I | 4.92E+0 | 3.57E-I | 2.28E+0 |
| | | 35 | 7.86E-I | 3.IIE+0 | 3.2IE-I | I.40E+0 |
| | | 40 | 4.26E+0 | I.23E+0 | I.54E-I | 5.39E-I |
| | | 45 | 7.03E+0 | 2.IIE-I | 2.88E-2 | 9.I4E-2 |
| | | 50 | 5.74E+0 | 6.86E-2 | 4.93E-3 | 3.I8E-2 |
| | | 55 | 3.00E+0 | 3.00E-I | 3.6IE-2 | I.32E-I |
| | | 60 | I.0IE+0 | 4.67E-I | 6.I0E-2 | 2.03E-I |
| | | 65 | I.87E-I | 4.34E-I | 5.72E-2 | I.89E-I |
| | | 70 | 6.52E-2 | 2.84E-I | 3.60E-2 | I.24E-I |
| E = 83.8 MeV | $\sigma_{\bar{p}p}$ = 199 mb, $\sigma_{\bar{p}n}$ = 157 mb<br>$B_{\bar{p}p} = B_{\bar{p}n}$ = 28.8 (GeV/c)$^{-2}$<br>$\varepsilon_{\bar{p}p} = \varepsilon_{\bar{p}n}$ = -0.09 | 5 | I.49E+3 | 3.24E+0 | 3.I5E+0 | 4.I6E-2 |
| | | I0 | I.04E+3 | 2.42E+0 | I.38E+0 | 5.I7E-I |
| | | I5 | 5.59E+2 | 3.60E+0 | I.80E-I | I.7IE+0 |
| | | 20 | 2.I4E+2 | 5.90E+0 | 5.06E-2 | 2.92E+0 |
| | | 25 | 4.84E+I | 6.6IE+0 | 3.64E-I | 3.I3E+0 |
| | | 30 | 2.45E+0 | 4.8IE+0 | 4.48E-I | 2.I8E+0 |
| | | 35 | 2.37E+0 | 2.I0E+0 | 2.50E-I | 9.22E-I |
| | | 40 | 6.65E+0 | 3.67E-I | 5.I0E-2 | I.58E-I |
| | | 45 | 5.73E+0 | 2.2IE-2 | I.86E-3 | I.0IE-2 |
| | | 50 | 2.72E+0 | 3.I3E-I | 4.23E-2 | I.36E-I |
| | | 55 | 6.80E-I | 5.IIE-I | 7.I2E-2 | 2.20E-I |
| | | 60 | 3.88E-2 | 4.28E-I | 5.87E-2 | I.85E-I |
| | | 65 | 5.9IE-2 | 2.25E-I | 2.87E-2 | 9.8IE-2 |
| | | 70 | I.59E-I | 6.87E-2 | 7.I0E-3 | 3.08E-2 |

| Energy | Parameters for $\bar{p}N$-amplitudes | Angle | Elastic scattering | Inelastic scattering (with exitation of $2^+$(4.44 MeV)-level) | | |
|---|---|---|---|---|---|---|
| | | $\theta^o_{cm}$ | $\frac{d\sigma^{el}}{d\Omega_{cm}}$, $\frac{mb}{sr}$ | $\frac{d\sigma}{d\Omega_{cm}}$, $\frac{mb}{sr}$ | $\frac{d\sigma_0}{d\Omega_{cm}}$, $\frac{mb}{sr}$ | $\frac{d\sigma_2}{d\Omega_{cm}}$, $\frac{mb}{sr}$ |
| E = 100.4 MeV | $\sigma_{\bar{p}p}$ = 188 mb, $\sigma_{\bar{p}n}$ = 149 mb<br>$B_{\bar{p}p} = B_{\bar{p}n}$ = 26.9 (GeV/c)$^{-2}$<br>$\varepsilon_{\bar{p}p} = \varepsilon_{\bar{p}n}$ = -0.07 | 5 | I.63E+3 | 3.65E+0 | 3.3IE+0 | 6.54E-2 |
| | | I0 | I.07E+3 | 2.86E+0 | I.30E+0 | 7.8IE-I |
| | | I5 | 5.I4E+2 | 4.88E+0 | 7.IIE-2 | 2.40E+0 |
| | | 20 | I.60E+2 | 7.55E+0 | I.74E-I | 3.69E+0 |
| | | 25 | 2.25E+I | 7.26E+0 | 5.25E-I | 3.37E+0 |
| | | 30 | I.4IE-I | 4.IIE+0 | 4.40E-I | I.84E+0 |
| | | 35 | 5.88E+0 | I.I0E+0 | I.43E-I | 4.8IE-I |
| | | 40 | 7.I3E+0 | 2.24E-2 | 3.I7E-3 | 9.62E-3 |
| | | 45 | 3.76E+0 | 2.55E-I | 3.46E-2 | I.I0E-I |
| | | 50 | 9.62E-I | 5.70E-I | 8.07E-2 | 2.45E-I |
| | | 55 | 4.79E-2 | 5.03E-I | 6.98E-2 | 2.I6E-I |
| | | 60 | 6.85E-2 | 2.47E-I | 3.I7E-2 | I.08E-I |
| | | 65 | I.79E-I | 6.03E-2 | 5.86E-3 | 2.72E-2 |
| | | 70 | I.63E-I | 2.50E-3 | 2.43E-4 | I.I3E-3 |
| E = 115.1 MeV | $\sigma_{\bar{p}p}$ = 176 mb, $\sigma_{\bar{p}n}$ = 145 mb<br>$B_{\bar{p}p} = B_{\bar{p}n}$ = 23.8 (GeV/c)$^{-2}$<br>$\varepsilon_{\bar{p}p} = \varepsilon_{\bar{p}n}$ = -0.05 | 5 | I.69E+3 | 4.05E+0 | 3.88E+0 | 8.8IE-2 |
| | | I0 | I.07E+3 | 3.32E+0 | I.27E+0 | I.02E+0 |
| | | I5 | 4.69E+2 | 6.04E+0 | 2.6IE-2 | 3.0IE+0 |
| | | 20 | I.24E+2 | 8.88E+0 | 2.94E-I | 4.29E+0 |
| | | 25 | I.08E+I | 7.63E+0 | 6.29E-I | 3.50E+0 |
| | | 30 | I.46E+0 | 3.57E+0 | 4.IIE-I | I.58E+0 |
| | | 35 | 7.63E+0 | 5.97E-I | 8.24E-2 | 2.57E-I |
| | | 40 | 6.30E+0 | 3.28E-2 | 3.58E-3 | I.46E-2 |
| | | 45 | 2.33E+0 | 4.94E-I | 6.92E-2 | 2.I2E-I |
| | | 50 | 2.94E-I | 6.64E-I | 9.43E-2 | 2.85E-I |
| | | 55 | I.72E-2 | 4.I6E-I | 5.63E-2 | I.80E-I |
| | | 60 | I.70E-I | I.3IE-I | I.50E-2 | 5,8IE-2 |
| | | 65 | I.93E-I | 9.90E-3 | 3.63E-4 | 4.77E-3 |
| | | 70 | I.IIE-I | 9.39E-3 | 3.02E-3 | 3.I8E-3 |

| Energy | Parameters for $\bar{p}N$-amplitudes | Angle | Elastic scattering | Inelastic scattering (with exitation of $2^+$(4.44 MeV)-level) | | |
|---|---|---|---|---|---|---|
| | | $\theta^\circ_{cm}$ | $\frac{d\sigma^{el}}{d\Omega_{cm}}, \frac{mb}{sr}$ | $\frac{d\sigma}{d\Omega_{cm}}, \frac{mb}{sr}$ | $\frac{d\sigma_0}{d\Omega_{cm}}, \frac{mb}{sr}$ | $\frac{d\sigma_2}{d\Omega_{cm}}, \frac{mb}{sr}$ |
| E = 128.5 MeV | $\sigma_{\bar{p}p}$ = 173 mb, $\sigma_{\bar{p}n}$ = 133 mb<br>$B_{\bar{p}p} = B_{\bar{p}n}$ = 25.2 (GeV/c)$^{-2}$<br>$\varepsilon_{\bar{p}p} = \varepsilon_{\bar{p}n}$ = 0.01 | 5 | I.82E+3 | 4.06E+0 | 3.82E+0 | I.20E-I |
| | | I0 | I.08E+3 | 3.67E+0 | I.0IE+0 | I.33E+0 |
| | | I5 | 4.23E+2 | 7.25E+0 | 5.3IE-4 | 3.63E+0 |
| | | 20 | 8.84E+I | 9.68E+0 | 4.64E-I | 4.6IE+0 |
| | | 25 | 2.98E+0 | 6.93E+0 | 6.49E-I | 3.I4E+0 |
| | | 30 | 4.09E+0 | 2.33E+0 | 2.80E-I | I.02E+0 |
| | | 35 | 7.88E+0 | I.I7E-I | I.53E-2 | 5.08E-2 |
| | | 40 | 4.24E+0 | 2.30E-I | 3.42E-2 | 9.8IE-2 |
| | | 45 | 8.95E-I | 6.34E-I | 9.35E-2 | 2.70E-I |
| | | 50 | 9.I5E-3 | 5.08E-I | 7.I8E-2 | 2.I8E-I |
| | | 55 | I.I0E-I | I.89E-I | 2.33E-2 | 8.30E-2 |
| | | 60 | I.76E-I | 2.08E-2 | I.23E-3 | 9.80E-3 |
| | | 65 | I.08E-I | 4.67E-3 | 2.0IE-3 | I.33E-3 |
| | | 70 | 3.49E-2 | 2.7IE-2 | 6.I5E-3 | I.05E-2 |
| E = 140.9 MeV | $\sigma_{\bar{p}p}$ = 162 mb, $\sigma_{\bar{p}n}$ = 139 mb<br>$B_{\bar{p}p} = B_{\bar{p}n}$ = 23.3 (GeV/c)$^{-2}$<br>$\varepsilon_{\bar{p}p} = \varepsilon_{\bar{p}n}$ = 0.15 | 5 | I.92E+3 | 4.56E+0 | 4.26E+0 | I.52E-I |
| | | I0 | I.09E+3 | 4.3IE+0 | I.0IE+0 | I.65E+0 |
| | | I5 | 3.94E+2 | 8.6IE+0 | I.20E-2 | 4.30E+0 |
| | | 20 | 6.84E+I | I.08E+I | 5.90E-I | 5.08E+0 |
| | | 25 | I.03E+0 | 6.84E+0 | 6.79E-I | 3.08E+0 |
| | | 30 | 6.88E+0 | I.80E+0 | 2.23E-I | 7.88E-I |
| | | 35 | 8.26E+0 | 5.05E-2 | 4.I0E-3 | 2.32E-2 |
| | | 40 | 3.32E+0 | 4.95E-I | 6.99E-2 | 2.I3E-I |
| | | 45 | 4.32E-I | 7.76E-I | I.IIE-I | 3.32E-I |
| | | 50 | 5.08E-2 | 4.59E-I | 6.20E-2 | I.99E-I |
| | | 55 | 2.I0E-I | I.I6E-I | I.26E-2 | 5.I9E-2 |
| | | 60 | I.85E-I | 8.66E-3 | I.I8E-3 | 3.74E-3 |
| | | 65 | 7.77E-2 | 2.69E-2 | 6.44E-3 | I.02E-2 |
| | | 70 | I.54E-2 | 4.34E-2 | 8.46E-3 | I.75E-2 |

| Energy | Parameters for $\bar{p}N$-amplitude | Angle | Elastic scattering | Inelastic scattering (with exitation of $2^+$(4.44 MeV)-level) | | |
|---|---|---|---|---|---|---|
| | | $\Theta^\circ_{cm}$ | $\frac{d\sigma^{el}}{d\Omega_{cm}}, \frac{mb}{sr}$ | $\frac{d\sigma}{d\Omega_{cm}}, \frac{mb}{sr}$ | $\frac{d\sigma_0}{d\Omega_{cm}}, \frac{mb}{sr}$ | $\frac{d\sigma_2}{d\Omega_{cm}}, \frac{mb}{sr}$ |
| E = 152.6 MeV | $\sigma_{\bar{p}p}$ = 157 mb, $\sigma_{\bar{p}n}$ = 142 mb<br>$B_{\bar{p}p} = B_{\bar{p}n}$ = 21.0 (GeV/c)$^{-2}$<br>$\varepsilon_{\bar{p}p} = \varepsilon_{\bar{p}n}$ = 0.10 | 5 | I.96E+3 | 4.96E+0 | 4.60E+0 | I.82E-I |
| | | I0 | I.08E+3 | 4.86E+0 | 9.83E-I | I.94E+0 |
| | | I5 | 3.64E+2 | 9.78E+0 | 3.49E-2 | 4.87E+0 |
| | | 20 | 5.30E+I | I.I6E+I | 7.08E-I | 5.45E+0 |
| | | 25 | 2.39E-I | 6.68E+0 | 7.03E-I | 2.99E+0 |
| | | 30 | 8.47E+0 | I.37E+0 | I.80E-I | 5.95E-I |
| | | 35 | 7.86E+0 | 3.65E-2 | 3.30E-3 | I.66E-2 |
| | | 40 | 2.45E+0 | 6.85E-I | 9.73E-2 | 2.94E-I |
| | | 45 | I.53E-I | 8.25E-I | I.I7E-I | 3.54E-I |
| | | 50 | I.08E-I | 3.84E-I | 5.02E-2 | I.67E-I |
| | | 55 | 2.5IE-I | 5.94E-2 | 5.33E-3 | 2.70E-2 |
| | | 60 | I.6IE-I | 7.39E-3 | 2.49E-3 | 2.45E-3 |
| | | 65 | 4.76E-2 | 4.26E-2 | 9.23E-3 | I.67E-2 |
| | | 70 | 4.20E-3 | 4.88E-2 | 8.78E-3 | 2.00E-2 |
| E = 163.7 MeV | $\sigma_{\bar{p}p}$ = 157 mb, $\sigma_{\bar{p}n}$ = 136 mb<br>$B_{\bar{p}p} = B_{\bar{p}n}$ = 22.2 (GeV/c)$^{-2}$<br>$\varepsilon_{\bar{p}p} = \varepsilon_{\bar{p}n}$ = 0.04 | 5 | 2.07E+3 | 4.97E+0 | 4.52E+0 | 2.25E-I |
| | | I0 | I.09E+3 | 5.38E+0 | 7.67E-I | 2.3IE+0 |
| | | I5 | 3.25E+2 | I.09E+I | I.I0E-I | 5.42E+0 |
| | | 20 | 3.52E+I | I.I7E+I | 8.28E-I | 5.42E+0 |
| | | 25 | 9.39E-I | 5.52E+0 | 6.I5E-I | 2.45E+0 |
| | | 30 | 9.55E+0 | 6.59E-I | 8.73E-2 | 2.86E-I |
| | | 35 | 6.23E+0 | I.6IE-I | 2.33E-2 | 6.9IE-2 |
| | | 40 | I.24E+0 | 8.I6E-I | I.20E-I | 3.48E-I |
| | | 45 | 4.76E-3 | 6.54E-I | 9.22E-2 | 2.8IE-I |
| | | 50 | I.82E-I | I.9IE-I | 2.27E-2 | 8.42E-2 |
| | | 55 | 2.06E-I | 6.35E-3 | I.IIE-4 | 3.I2E-3 |
| | | 60 | 8.43E-2 | 2.25E-2 | 6.00E-3 | 8.25E-3 |
| | | 65 | I.23E-2 | 4.50E-2 | 8.89E-3 | I.8IE-2 |
| | | 70 | I.87E-4 | 3.I0E-2 | 5.I4E-3 | I.29E-2 |

Т - 04752

Подписано в печать 7 марта 1984 года

Заказ № 137. Тираж 100 экз. п/л 1,2

Отпечатано в Отделе научно-технической информации ФИАН СССР

Москва, В-312, Ленинский проспект, 53